

## American Journal of Scientific Research and Essays (ISSN:2475-7527)



# Design and adaptive control of omni-directional mobile platform with four driving wheels

**Weibin Zhang**

School of Mechanical Engineering, Jiangsu University of Science and Technology, Zhenjiang 212003, P.R. China

### ABSTRACT

In this paper, a general kinematic model of the four drive wheel omnidirectional mobile platform is established, and the CMAC (Cerebellar model articulation controller) +PID joint control strategy is used to design the embedded adaptive control of the omnidirectional mobile platform in view of the problem that the conventional control can not be self-tuning online and the real-time response of the response needs to be improved. The MATLAB simulation and experimental analysis of DC motor speed regulation were carried out, and the motion performance of the prototype was tested by a series of typical experiments. The results show that the kinematic model of the mecanum wheel omnidirectional moving platform is reasonable. The dynamic response of the CMAC+PID adaptive controller is fast, the control precision is high, and the robustness is good. The prototype can achieve the horizontal / vertical translation, the original rotation and the omni-directional motion in the plane. The overall performance can meet the requirements of the engineering application.

**Keywords:** mecanum wheel; omni-directional movement platform; kinematics analysis; CMAC+PID controller

### \*Correspondence to Author:

Weibin Zhang  
School of Mechanical Engineering,  
Jiangsu University of Science and  
Technology, Zhenjiang 212003, P.R.  
China

### How to cite this article:

Weibin Zhang. Design and adaptive control of omni-directional mobile platform with four driving wheels. American Journal of Scientific Research and Essays, 2018 3:7. DOI: 10.28933/ajsre-2018-06-2801



eSciPub LLC, Houston, TX USA.

Website: <http://escipub.com/>

## Introduction

Wheeled mobile is currently the most widely used mobile form. The omnidirectional wheeled mobile system has 3 degrees of freedom in the plane without changing its position and posture, and can realize vertical translation, lateral displacement, original rotation and arbitrary combination. Compared with the traditional wheel movement, the omnidirectional wheel movement has the characteristics of small operating space, high working efficiency and zero turning radius. It is especially suitable for small crowded or closed operation situations and has been applied gradually in the fields of life service, storage and transportation and so on.

Kinematics modeling of omnidirectional mobile platform is the theoretical basis for analyzing whether it can achieve omnidirectional motion, and is also an inevitable requirement for its motion control [1-3]. At present, there are two ways to establish the omnidirectional platform kinematics models: matrix transformation method and vector analysis method. In the literature, the matrix transformation method is used to establish the plane kinematics model, which is simple and easy to understand. However, because of the use of scalar analysis, the generality and intuition are poor, and the method is completely invalid when establishing the uneven ground motion model.

Omni-directional mobile platform mainly relies on omnidirectional wheel group to realize omnidirectional mobile. Omnidirectional wheels include ball wheel, continuous switch wheel, orthogonal wheel, mecanum wheel and so on. Among them, the mecanum wheel has attracted more and more attention due to its simple structure and flexible motion<sup>[4]</sup>. Its multi wheel cooperative motion control has become a hot topic in recent years. At present, the algorithms

used in the motion control of omnidirectional platform mainly include conventional PID control and fuzzy PID control<sup>[5-6]</sup>. In document [7], the omnidirectional movement control of the robot is realized by conventional PID algorithm, but its control parameters are set off under certain conditions in advance, so the motion effect is often not ideal in the actual operation of the platform because of the possible changes in the condition of the pavement. In literature [8], the fuzzy PID self-tuning algorithm is adopted. Although it can dynamically adjust the PID control parameters according to the change of the road condition, it will affect the real-time response of the platform because of its complicated program, especially when the running speed is fast, it may cause its instantaneous deviation from the planned motion path due to the existence of the body inertia. The cerebellar model controller (Cerebellar model articulation controller, CMAC) is a form query adaptive neural network for simulating the function of the human body. The local generalization ability is strong and the convergence speed is fast. It can better overcome the error of the regular PID controller in controlling the nonlinear system and the complexity of the fuzzy PID algorithm and the response of the fuzzy PID algorithm<sup>[9-10]</sup>. The disadvantages of slow speed can be used for real-time control of omni-directional platforms under complex conditions such as inadequate environment and uncertain factors.

Taking the mecanum wheel omnidirectional moving platform as the research object, based on the analysis of its omnidirectional motion principle, the inverse kinematics model is established by vector analysis. The CMAC+PID adaptive joint controller is designed based on the cerebellar model neural network and the conventional PID control algorithm, and the

controller is used to adjust the DC motor<sup>[11]</sup>. The MATLAB simulation and experimental analysis are carried out at the same time. Finally, the motion performance of the prototype is tested and evaluated. The results show that the established kinematics model is reasonable. The simulation and measurement results of the CMAC+PID joint control algorithm are good, which can meet the requirements of the control precision, real-time and stability of the platform in the engineering application.

### Principle of omni-directional movement

Fig. 1 is the basic structure of the mecanum wheel, which is mainly made up of parts such as rollers, supports, wheels and so on. Its structure is characterized by the installation of a number of drum shaped rollers with a fixed offset angle

on the axis of the wheel in the circumference of the wheel, and the roller can be freely rotated. The outer contour of the roller is approximately enveloped into a cylinder, and at least one roller contacts with the ground at any time to ensure continuity and smoothness of motion. In the buffer material of each roller including a peripheral layer of hard rubber to reduce wear and motion noise of the roller, and reduce the requirement for mecanum wheel installation. The special structure of the mecanum wheel makes each wheel rotate around the axis of the hub under the drive of the motor, and can also move along the axis of the roller along the axis of the roller along the axis of the surrounding roller.

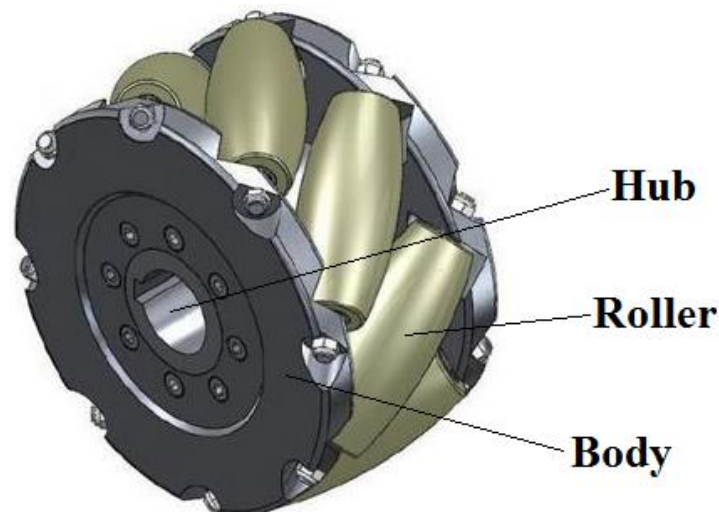


**Fig.1 Outline structure of mecanum wheel**

The object of this study is a omnidirectional mobile platform consisting of four mecanum wheels. As shown in Figure 2, it uses a four wheel drive, that is, each mecanum wheel is driven independently by the corresponding DC motor through a reducer. In the course of the platform, the speed and steering of each DC motor are controlled by Microcontroller unit (MCU), so that the platform can realize the basic movement of horizontal / longitudinal

translational, in-situ rotation and all kinds of complex combinations in the plane. Each mecanum wheel is connected with the vehicle body through the corresponding cantilever frame. Considering that the actual pavement may be partially uneven, spring shock absorbers are used to make every moment of the wheel contact with the ground and reduce the knocking of the wheel on the ground to ensure the accuracy and stability of the platform.

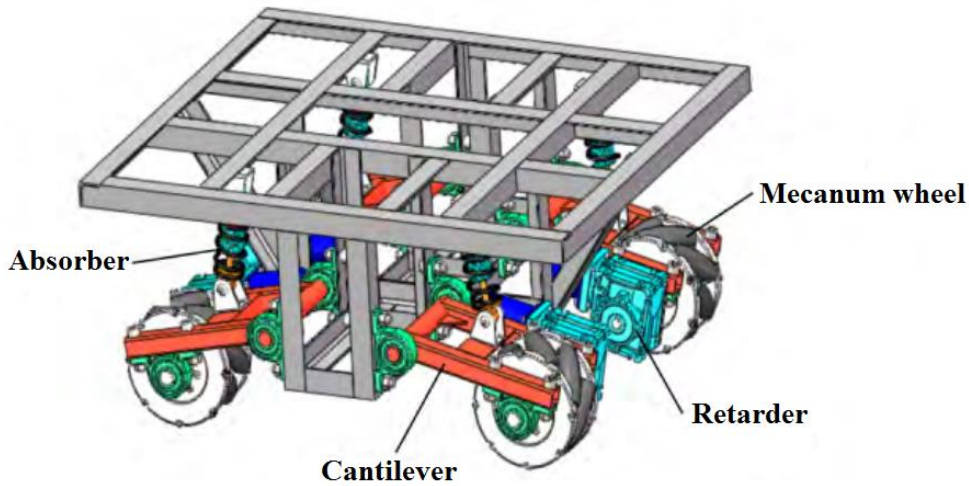


**Fig.2 Omni-directional mobile platform with four driving wheels**

To simplify the analysis, the following assumption is made: the car body is rigid, neglecting slight stress and deformation; the contact between the roller and the ground is only pure rolling without relative sliding.

Figure 3 shows the force analysis of the platform when it is moving sideways and rotating in situ. The diagram shows the actual bias direction of the ground roller;  $\omega_1 \sim \omega_4$  is the rotation angular velocity of each wheel, the size is the same, the direction and the actual steering of the wheel are in the right hand rule. When the mecanum wheel rotates, the friction force produced by the ground roller and the ground is opposite to the moving direction of the place

wheel. The friction force is decomposed into the axial friction force  $F_a$  along the roller axis and the rolling friction  $F_r$  perpendicular to the roller axis, the former is the main force of the movement of the driving platform, and the latter is relatively small, usually available. Ignore. In Fig.3(a), the force of the force  $F_a$  of each ground roller is decomposed horizontally and longitudinally, then the force in the longitudinal direction of the front and rear wheels of the platform will counteract each other, and the 4 lateral forces make the platform move laterally right. The force of the wheel in Fig.3(b) will make the platform rotate clockwise around its center  $O$ , that is, the original rotation (zero turning radius).

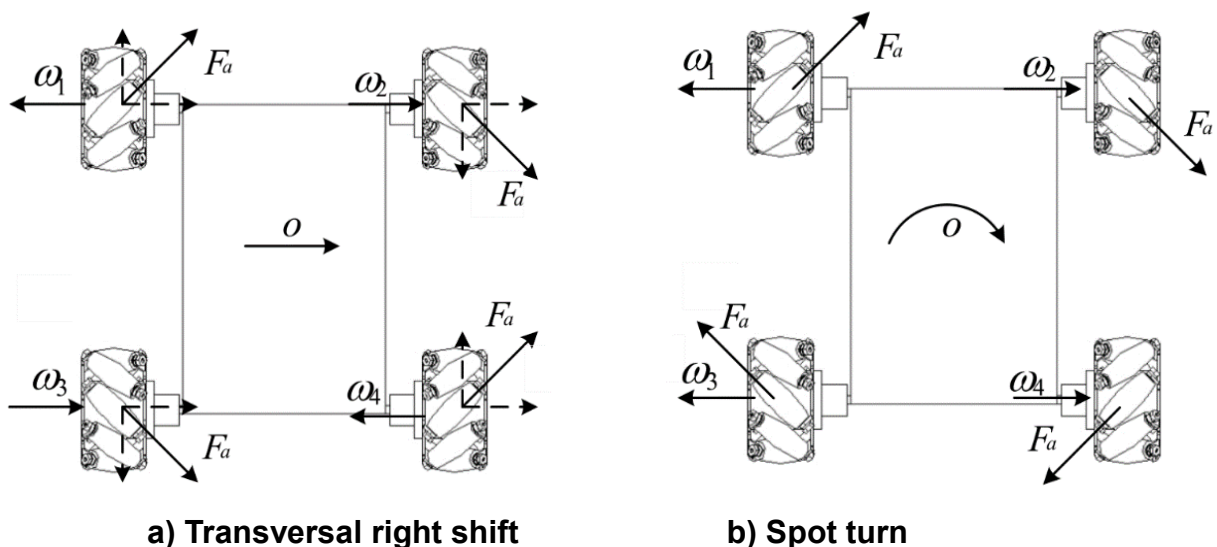


**Fig.3 Force analysis of omni-directional mobile platform**

**Kinematics analysis and wheel set layout**

**Establishment of inverse kinematics model**

The establishment of platform inverse kinematics model is the theoretical basis for its motion control. By using the vector analysis method, the basic idea is: first from the mecanum single wheel, the velocity expression of the center point of the roller center point  $R_i$  to the center point of the mecanum wheel is listed, and then the expression of the velocity of the center point of the center of mass to the center point  $O'_i$  of the Mecanum wheel is analyzed from the whole platform, and the above expression is set up and simplified, The velocity mapping relationship between the four wheels and the center of mass of the platform is derived, that is, the kinematic model of the

omnidirectional platform.

Fig. 4 is the structural schematic diagram of the No. $i$  mecanum wheel. Among them,  $r$  and  $r_1$  are the radius of the mecanum wheel and the roller;  $e_i$  and  $g_i$  are the unit vectors in the axis of the wheel hub and the axis direction of the roller respectively;  $P_i$  is the contact point between the ground roller and the ground, and a straight line that intersects the axis of the wheel hub and the axis of the roller, and the intersection points are  $R_i$  and  $O'_i$  respectively. These two points are roller and wheel. The center of the hub  $i, j$  is the unit vector in the direction of the  $O'_i R_i$ ;  $f_i$  and  $h_i$  are the unit vectors of the vertical axis and  $O'_i R_i$ , respectively;  $\dot{\theta}_i$  and  $\dot{\phi}_i$  are the wheels and roller speeds respectively.

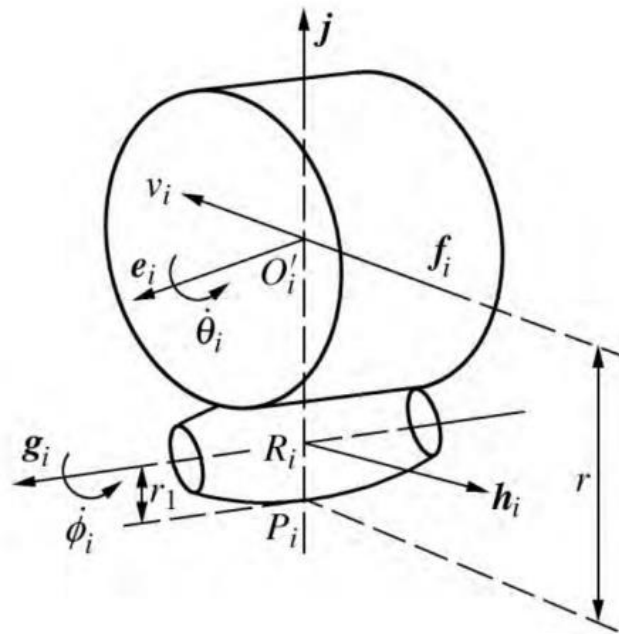


**Fig.4 Structure diagram of the No. $i$  mecanum wheel**

First relate the line speed  $\dot{O}'_i$  of the hub's center point to the line speed  $\dot{R}_i$  of the center point of the ground roller:

$$\dot{O}'_i = \dot{R}_i + v_i \tag{1}$$

$$v_i = (\omega_j + \dot{\theta}_i e_i) \times (r - r_1) j = -\dot{\theta}_i (r - r_1) f_i \tag{2}$$

$$\dot{R}_i = (\omega_j + \dot{\theta}_i e_i + \dot{\phi}_i g_i) \times r_1 j = -r_1 (\dot{\theta}_i f_i + \dot{\phi}_i h_i) \tag{3}$$

The (1) ~ (3) type of joint can be obtained.

$$\dot{O}'_i = -r \dot{\theta}_i f_i - r_1 \dot{\phi}_i h_i \tag{4}$$

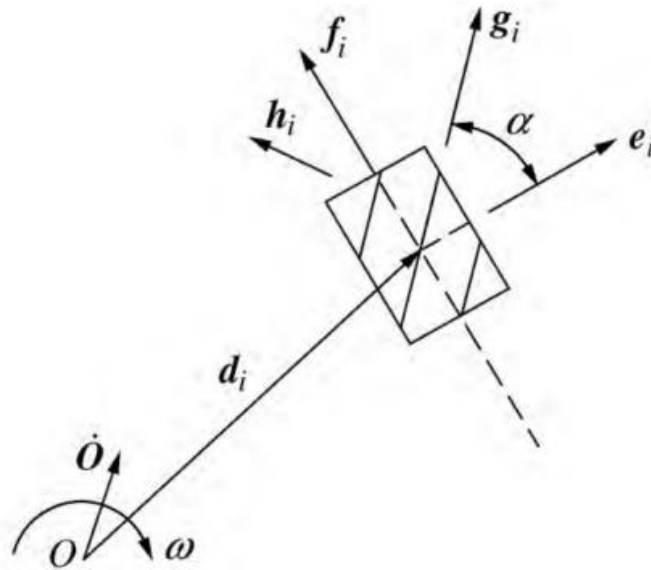


**Fig.5 The relationship between the No.i mecanum wheel and center point O**

Then we discuss the speed expression of the mecanum hub  $O'_i$  relative to the  $O$  point of the platform center. Figure 5 describes the relationship between the No.i mecanum wheel and the mobile platform  $O$ .

$$\dot{O}'_i = \dot{O} + \omega E d_i \tag{5}$$

In the formula,  $\dot{O}$  and  $\omega$  are the linear velocity and rotation angular velocity of the center of the flat platform, which is called the generalized velocity, and the  $d_i$  is the position vector of the center point  $O$  of the moving platform to the center point  $O'_i$  of the wheel  $i$ ;  $E$  is the rotation matrix that rotates 90 degrees against the  $d_i$  counter clockwise.

Because all rollers are not driven, they are inert, so  $\dot{\phi}$  can be eliminated. The left and right sides of the formula (4) and (5) are multiplied by  $h_i^T$ , and can derive:

$$\dot{\theta}_i = -\frac{1}{r \sin \alpha} \left( h_i^T \quad h_i^T g E d_i \right) \begin{pmatrix} \dot{O} \\ \omega \end{pmatrix} \tag{6}$$

$\alpha$  is the offset angle of the roller axis relative to the hub axis. If we consider the relationship

between the 4 mecanum wheels, we can establish the general form of the inverse kinematics model for omni directional platform control.

$$\dot{\theta} = \begin{pmatrix} \dot{\theta}_1 \\ \dot{\theta}_2 \\ \dot{\theta}_3 \\ \dot{\theta}_4 \end{pmatrix} = -\frac{1}{r \sin \alpha} K \begin{pmatrix} \dot{O} \\ \omega \end{pmatrix} = -\frac{1}{r \sin \alpha} \begin{pmatrix} h_1^T & h_1^T \bullet E d_1 \\ h_2^T & h_2^T \bullet E d_2 \\ h_3^T & h_3^T \bullet E d_3 \\ h_4^T & h_4^T \bullet E d_4 \end{pmatrix} \begin{pmatrix} \dot{O} \\ \omega \end{pmatrix} \tag{7}$$

$\dot{\theta}$  is the rotation speed of 4 mecanum wheels (including steering);  $K$  is the jacobian matrix of the control model.

It can be seen that if the omni-directional platform is required to move according to different paths or rules, the generalized velocity of the center will change at any time. After determining the layout of the wheel group and the offset angle of the roller, through the formula (7), the corresponding speed of 4 wheels can be calculated in real time, and the transmission ratio of the reducer is considered, and MCU can realize the expected full movement of the platform through the coordinated control of the speed of 4 DC motors.

## Optimal wheel set layout

Theoretically, there are many forms of wheel group layout for the four round platform<sup>[12]</sup>. But it is not arbitrary layout that can achieve all-around movement in the plane<sup>[13]</sup>. In practical

applications, the 4 mecanum wheels generally adopt two left and two right-handed group pairs, and rank ( $K$ ) =3 is the precondition for realizing omnidirectional motion. This paper selects two kinds of full rank structures as shown in Figure 6.

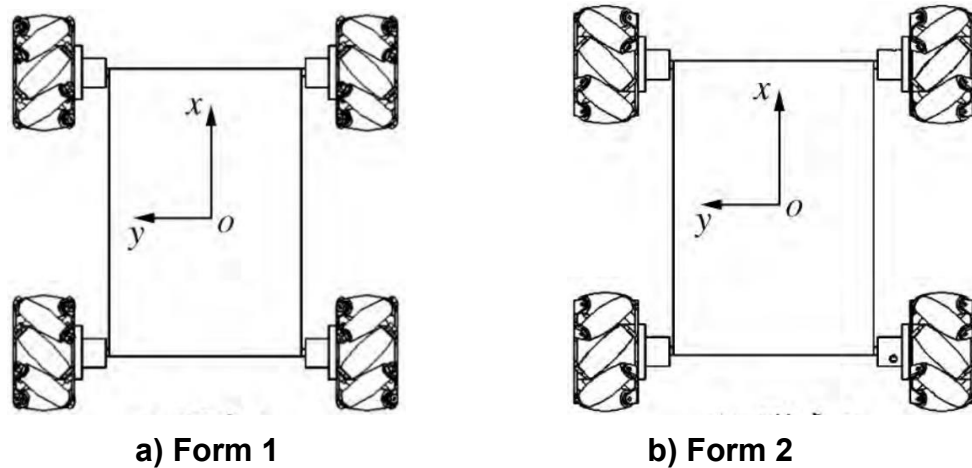


**Fig.6 Typical wheel group layout structure of omnidirectional platform**

Further analysis shows that rank ( $K$ ) = 3 is not a sufficient condition for the realization of the omnidirectional movement of the platform, that is, the above two kinds of layout do not necessarily ensure that the platform performs all directional movement in the plane. For figure 6a), if the size of each center of the 4 wheels is just square and the offset angle of the roller is equal, the direction of the 4 wheels center points is exactly the O point of the center of the platform, causing the platform to be unable to achieve the rotation movement around its center point. So in this case, figure 6b) is the best structural form of the four round omnidirectional mobile platform wheel group layout.

## Design of the adaptive controller

### DC motor speed regulation model

According to the requirements of the bearing capacity and speed of the mobile platform, the brushless DC motor 57BL75S10 is selected for each wheel group, and the mecanum wheel is driven by the reducer. The control input is  $U$  of

the armature voltage and the output is  $w$  of the angular velocity of the motor. According to the modeling method described in document [14], the corresponding transfer function of the DC motor can be derived as equation (8)

$$G(s) = \frac{U(s)}{W(s)} = \frac{K_M}{(L_s + R)(J_s + B) + K_M K_E} \quad (8)$$

where,  $R$  and  $L$  are the resistance and inductance of the armature,  $K_E$  is electromotive force constant,  $K_M$  is electromagnetic torque coefficient,  $B$  is viscous friction coefficient, and the moment of inertia is denoted as  $J$ .

### CMAC+PID combined control strategy

The cerebellar model controller CMAC is a nonlinear associative neural network based on local learning in the human cerebellum, which has the characteristics of small computation, fast learning speed and strong local generalization ability<sup>[15-16]</sup>. The CMAC model structure is shown in Figure 7, which is composed of the input state space  $S$ , the concept memory  $A$ , the actual

memory  $A_1$  and the output  $Y$ . It includes two mappings:  
 1) Concept mapping ( $S \rightarrow A$ ): mapping each input  $n$ -dimensional vector in  $S$  to the  $A$  of concept memory and activating  $c$  units in  $A$ . In  $S$ , two adjacent input vectors will stimulate some overlapping elements in  $A$ . The closer the

distance, the more overlap, that is, local generalization.  
 2) Actual mapping ( $A \rightarrow A_1$ ): mapped  $C$  units in  $A$  to  $C$  units of  $A_1$  by stray coding technology, and CMAC output to the sum of connection weights stored in the  $C$  units of  $A_1$ .

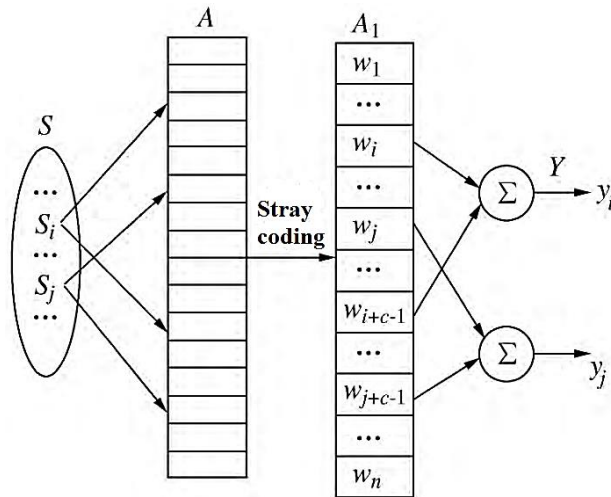


**Fig.7 Basic structure of CMAC**

In this paper, a CMAC+PID joint control strategy is adopted for platform speed control, and its structure is shown in Figure 8. The CMAC controller mainly realizes the feedforward control to ensure the response speed of the motor speed control, but because of its poor robustness, the conventional PID controller is introduced to realize feedback control<sup>[17-18]</sup>. In

order to improve the rashness of the platform speed control, it can effectively suppress the external disturbance and ensure the stability of the operation. The joint control effect of CMAC+PID is not very closely related to the 3 control parameters in PID, and only requires them to be within reasonable limits.

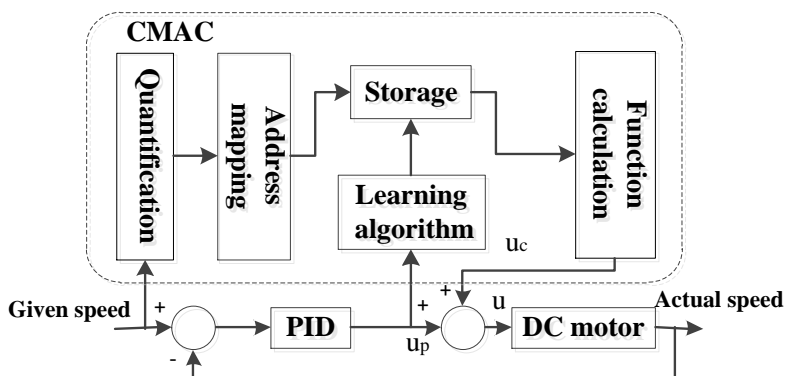


**Fig.8 Joint control structure of CMAC+PID**



The control signal is generated by CMAC and conventional PID. When the motor starts running, the CMAC ownership value is 0, and the PID controller is controlled at this time. At the same time, the PID controller provides the tutor signal for the CMAC, and uses the PID output value  $u_p$  to train the connection weight of CMAC online<sup>[19-20]</sup>. At the same time, the given speed of the motor is quantized to CMAC, so as to find  $c$  units corresponding to it in the CMAC memory and add the connection weights in these units, the output  $u_c(k)$  of the CMAC can be obtained as equation (9)

$$u_c(k) = \sum_{i=1}^c w_i a_i \quad (9)$$

where,  $a_i$  is binary selection vector, if the No. $i$  storage cell is activated, then  $a_i = 1$ , otherwise it is zero;  $c$  is generalization parameter. The output is added to the PID controller output  $u_p(k)$  to get the total control input of the DC motor as equation (10).

$$u(k) = u_c(k) + u_p(k) \quad (10)$$

When CMAC maps the concept, the input space  $S$  is divided into  $N+2C$  quantization intervals in interval  $[S_1, S_2]$  as equation (11).

$$\begin{cases} d_1, \Lambda, d_c = S_1 \\ d_i = d_{i-1} + \Delta d_i, i = c + 1, \Lambda, c + N \\ d_{N+c+1}, \Lambda, d_{N+2c} = S_2 \end{cases} \quad (11)$$

CMAC realizes the actual mapping relationship by equation (12)

$$a_i = \begin{cases} 1, S_k \in [d_i, d_{i+c}], i = 1, N + c \\ 0, other \end{cases} \quad (12)$$

where,  $S_k$  is the No. $k$  input sample value.

### Performance testing

An experimental prototype of the mecanum wheel omnidirectional mobile platform is built. The main controller, MCU, selects STM32 single

The adjustment goal of the CMAC+PID joint control algorithm is shown as equation (13).

$$E(k) = \frac{1}{2} (u_c(k) - u(k))^2 \cdot \frac{1}{c} \quad (13)$$

The purpose is to make the final control signal of the system come from  $u_c$  completely. This not only improves the control accuracy of the four round platform, speeds up the response speed, but also enhances the robustness of the control. Gradient descent method is used to train CMAC weights. Formula (14)-(15) are the adjustment rules

$$\Delta w(k) = -\eta \frac{\partial E(k)}{\partial w} = \eta \frac{u(k) - u_c(k)}{c} a_i = \eta \frac{u_p(k)}{c} a_i \quad (14)$$

$$w(k) = w(k - 1) + \Delta w(k) + \alpha(w(k) - w(k - 1)) \quad (15)$$

where,  $\eta$  is the learning rate,  $0 < \eta < 1$ ;  $\alpha$  is the momentum factor.

### MATLAB simulation analysis

Simulation of single DC motor speed regulation based on MATLAB. Figure 9 describes the simulation response curve of the motor under two algorithms of CMAC+PID joint control and conventional PID control by applying a speed step signal to the foregoing motor, with a sampling time interval of 10ms. It can be seen that the rise time of the former is only 0.15s, and the latter is 0.35s, which indicates that the introduction of the cerebellum model makes the speed of motor speed up by more than half, and the speed of the motor response has been significantly improved and no overshoot. It is theoretically verified that the former has obvious effect on improving the speed response speed of DC motor.

### Test and result analysis of prototype

chip microcomputer to communicate with the upper PC by bluetooth, in order to debug easily. When the system runs, the PC machine first sends the control parameters including the

platform motion to the main controller in the form of the message, and then extracts the generalized velocity parameters immediately after the latter is received, and calculates the rotational angular velocity of the four wheel according to the inverse kinematics model, and then the main controller is at the same time at

the same time. The channel motor driver sends out corresponding PWM signals for cooperative control. When the DC motor is rotating, the real-time wheel speed can be fed back to the main controller through the photoelectric encoder installed at its tail, thus forming negative feedback control.

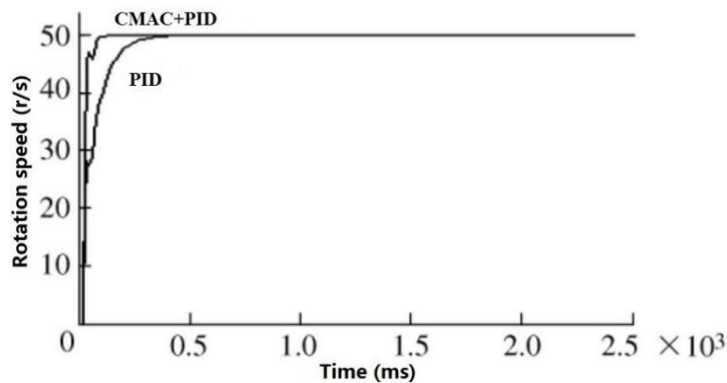


**Fig.9 Simulation of DC motor speed control**

In order to observe the actual effect of the speed control of the DC motor, the real-time speed of each motor can be converted to the voltage signal that can be captured by the digital oscilloscope by using the DAC module in the STM32 single chip microcomputer, thus the dynamic response curve of the motor speed control is obtained.

Fig.10 describes the measured step response curve of the DC motor under the two algorithms

of CMAC+PID combined control and conventional PID control. The sampling time interval is still 10s. It can be seen that the rise time of the measured response curve of the former is 0.19s, and the 0.4s of the former is significantly shorter than that of the latter, and it has no overshoot, which proves the validity of the former in improving the real-time performance of DC motor speed regulation.

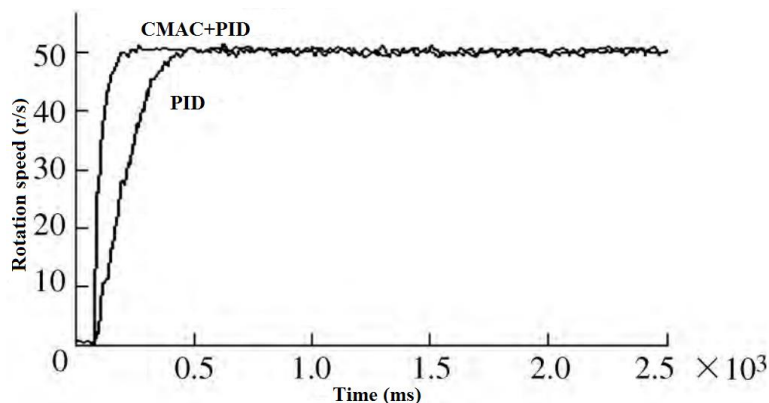


**Fig.10 Measured response characteristics of DC motor rotation speed control**

The comparison between Fig. 9 and Fig.10 shows that the simulation results are basically consistent with the measured ones, which indicates that the modeling results of the foregoing DC motor speed regulation are reasonable. However, the measured response speed of the motor is slightly slower than that of the MATLAB simulation, which is due to the inability to take into account all the factors such as the small mechanical friction in the motor and the actual conditions of the platform moving road, which are unavoidable in the experiment.

In order to further evaluate the overall motion performance of the prototype with CMAC+PID joint control strategy in control precision and stability, a multi group motion control experiment was carried out.

Fig.11 shows the trajectory of a prototype at a given speed  $v=10\text{cm/s}$  condition. The results show that the actual speed of the prototype is basically consistent with the theoretical speed, and the maximum error is  $0.21\text{cm/s}$ , and the prototype runs smoothly.

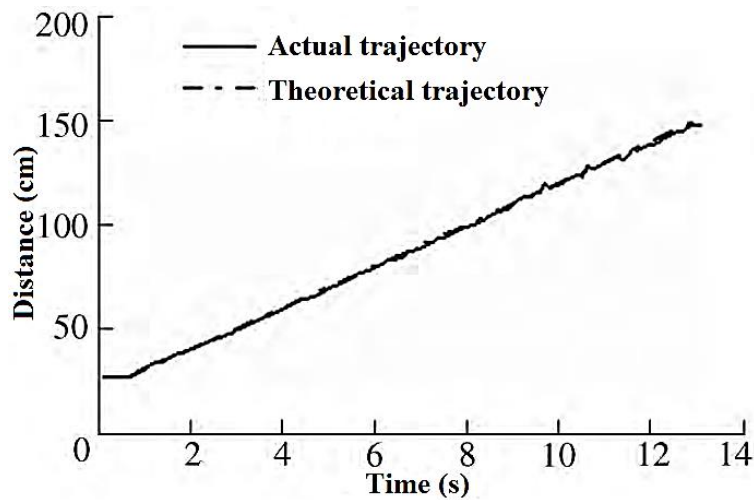


**Fig.11 Longitudinal motion trajectory**

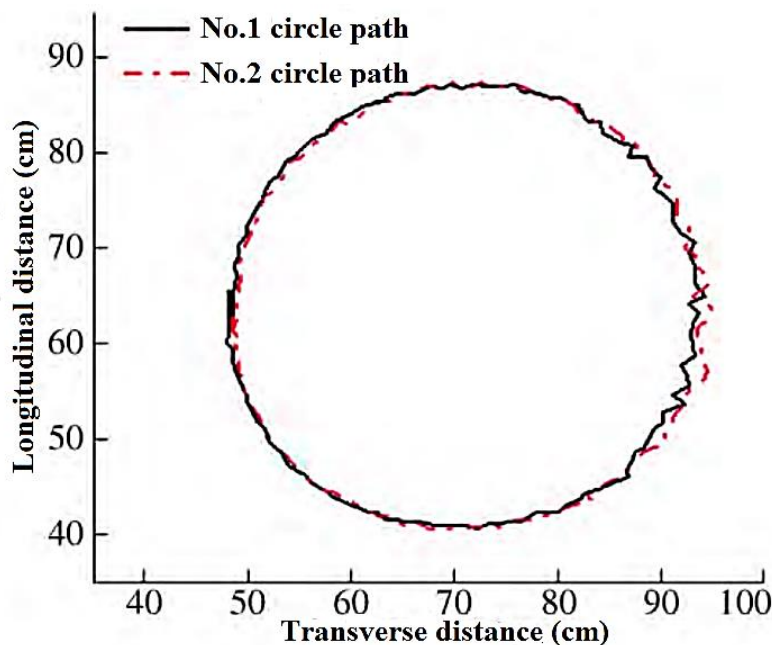


**Fig.12 Continuous circumference trajectory**

Fig.12 shows the measured curves for two consecutive circular trajectories. It can be seen that, due to the slight sliding of the wheel and the fine vibration of the car body, a small number of position deviations exist after the two-circle circular motion of the prototype, but the overall operation is basically stable and the repeatability of the trajectory can meet the practical application requirements of the project.

### **Result analysis**

1) As the periphery of the roller is wrapped with a layer of hard rubber material, the roller contact area will produce local micro deformation under the action of the moving platform itself and its external bearing, which leads to the actual effective radius of the mecanum wheel is less than the theoretical value, which will bring a certain error to the inverse kinematics model for the control of the mobile platform.

2) The fluctuation of the load torque caused by the switching of the rotation of the adjacent rollers at the moment of switching to the ground will bring a periodic small disturbance to the rotational speed of the wheel group; at the same time, in fact, the objective surface unevenness in the ground will also bring the "ground knocking" phenomenon that cannot be completely avoided for the mecanum wheel. However, the experiment shows that the CMAC+PID joint controller can still exhibit good response speed and steady state performance, and also improve the motion control accuracy of the mobile platform.

3) Because of the non-idealization of the experimental conditions, the assumptions made before the platform kinematic model are not fully satisfied, for example, the roller may appear non-pure rolling, and the error is unavoidable because of the mecanum wheel machining, the body and wheel set installation. At the same time,

the precision of the vehicle longitudinal / lateral distance measuring sensor is also limited. The above factors will bring adverse effects on the overall motion performance test of the prototype, such as the slight movement of the longitudinal motion of the platform, the trace motion of the transverse motion, and the existence of a small amount of sliding in the circular motion, which should be further improved.

### **Conclusion**

Based on the analysis of the mecanum wheel structure and the omnidirectional movement of the platform, the inverse kinematics model of the platform control is established on the basis of the analysis of the mecanum wheel structure and the principle of the platform omnidirectional movement. The embedded adaptive controller is designed based on the CMAC+PID joint control algorithm, and the simulation and reality of the DC motor speed control are carried out. Finally, the overall motion performance of the prototype is evaluated and analyzed through typical experiments such as longitudinal movement, lateral movement and multi circle motion. The simulation and experimental results show that the CMAC+PID joint controller has high control precision, fast response speed and good robustness. It can meet the requirements of engineering application. The platform can achieve all directional movement in the plane steadily and has the unique advantages of lateral displacement and original rotation. It is flexible and efficient in motion, high in space utilization, and should be used in engineering. It has a bright future.

### **ACKNOWLEDGMENT**

This work is supported by Jiangsu Provincial University Graduate Practical Innovation Project (SJLX15\_0524).

### **References**

1. Kim, H., & Kim, B. K., 2014, "Online minimum-energy trajectory planning and control on a straight-line path for three-wheeled omnidirectional mobile robots", *IEEE Transactions on Industrial Electronics*, 61(9), pp. 4771-4779.
2. Jia, Z. J., Song, Y. D., & Cai, W. C., 2013, "Bio-inspired approach for smooth motion control of wheeled mobile robots," *Cognitive Computation*, 5(2), pp. 252-263.
3. Kanjanawanishkul, K., 2015, "Omnidirectional wheeled mobile robots: wheel types and practical applications," *International Journal of Advanced Mechatronic Systems*, 6(6), pp. 289-302.
4. Sherback, M., Purwin, O., & D'Andrea, R., 2006, "Real-time motion planning and control in the 2005 cornell robocup system," *Robot Motion and Control*, pp. 245-263.
5. Bruce, J. R., 2006, "Real-time motion planning and safe navigation in dynamic multi-robot environments," (No. CMU-CS-06-181). CARNEGIE-MELLON UNIV PITTSBURGH PA SCHOOL OF COMPUTER SCIENCE.
6. Purwin, O., & D'Andrea, R., 2006, "Trajectory generation and control for four wheeled omnidirectional vehicles," *Robotics and Autonomous Systems*, 54(1), pp.13-22.
7. Juang, C. F., Lai, M. G., & Zeng, W. T., 2015, "Evolutionary fuzzy control and navigation for two wheeled robots cooperatively carrying an object in unknown environments," *IEEE transactions on cybernetics*, 45(9), pp. 1731-1743.
8. Chwa, D., 2012, "Fuzzy adaptive tracking control of wheeled mobile robots with state-dependent kinematic and dynamic disturbances," *IEEE transactions on Fuzzy Systems*, 20(3), pp. 587-593.
9. Yang, S. X., Zhu, A., Yuan, G., & Meng, M. Q. H., 2012, "A bioinspired neurodynamics-based approach to tracking control of mobile robots," *IEEE Transactions on Industrial Electronics*, 59(8), pp. 3211-3220.
10. Kayacan, E., Kayacan, E., Ramon, H., & Saeys, W., 2013, "Adaptive neuro-fuzzy control of a spherical rolling robot using sliding-mode-control-theory-based online learning algorithm," *IEEE transactions on cybernetics*, 43(1), pp. 170-179.
11. Gao, H., Song, X., Ding, L., Xia, K., Li, N., & Deng, Z., 2014, "Adaptive motion control of wheeled mobile robot with unknown slippage," *International Journal of Control*, 87(8), pp. 1513-1522.
12. Hoang, N. B., & Kang, H. J., 2016, "Neural network-based adaptive tracking control of mobile robots in the presence of wheel slip and external disturbance force," *Neurocomputing*, 188, pp. 12-22.
13. Boukens, M., & Boukabou, A., 2017, "Design of an intelligent optimal neural network-based tracking controller for nonholonomic mobile robot systems," *Neurocomputing*, 226, pp. 46-57.
14. Su, K. H., Chen, Y. Y., & Su, S. F., 2010, "Design of neural-fuzzy-based controller for two autonomously driven wheeled robot," *Neurocomputing*, 73(13), pp. 2478-2488.
15. Li, S., Wang, H., & Rafique, M. U., 2017, "A novel recurrent neural network for manipulator control with improved noise tolerance." *IEEE Transactions on Neural Networks and Learning Systems*.
16. Li, S., Zhang, Y., & Jin, L., 2016, "Kinematic control of redundant manipulators using neural networks," *IEEE transactions on neural networks and learning systems*.
17. Zhang, Y., & Li, S., 2017, "Predictive suboptimal consensus of multiagent systems with nonlinear dynamics," *IEEE Transactions on Systems, Man, and Cybernetics:Systems*.
18. Li, S., Zhou, M., Luo, X. & You, Z. H., 2017, "Distributed winner-take-all in dynamic networks," *IEEE Transactions on Automatic Control*, 62(2), pp.577-589.
19. Jin, L., Li, S., La, H.M. and Luo, X., 2017, "Manipulability optimization of redundant manipulators using dynamic neural networks," *IEEE Transactions on Industrial Electronics*.
20. Sheikhlar, A., Fakharian, A., Beik-Mohammadi, H., & Adhami-Mirhosseini, A., 2016, "Design and Implementation of Self-Adaptive PD Controller

Based on Fuzzy Logic Algorithm for Omni-Directional Fast Robots in Presence of Model Uncertainties,” International Journal of Uncertainty, Fuzziness and Knowledge-Based Systems, 24(05), pp. 761-780.

